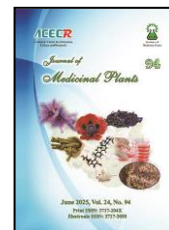




Institute of
Medicinal Plants

Journal of Medicinal Plants

Journal homepage: www.jmp.ir



Research Article

Synthesis, characterization, anti-microbial activity of silver nanoparticles, and molecular interaction studies of therapeutic agents of *Pongamia pinnata* (PP) and *Azadirachta indica* (AI)

M. S. Veena Anasthasia¹, C. Mansiya², V. Kannappan³, A. Justin Adaikala Baskar^{1,*}

¹Department of Chemistry, Loyola College, Chennai-600 034, India

²Department of Chemistry, SDNB Vaishnav College for Women, Chennai-600 044, India

³Department of Chemistry, Presidency College, Chennai-600 005, India

ARTICLE INFO

Keywords:

Nanomaterials
Phytochemical
Antimicrobial
Antidiabetic
In-Silico docking
analysis

ABSTRACT

Background: Antimicrobial activity has been reported against a range of bacteria, including multidrug-resistant strains for silver nanoparticles (AgNPs) due to penetration of NPs into the cell. AgNPs can be used in combination with other antibacterial agents to create a synergistic effect. **Objective:** The present work aims at the preparation of AgNPs in methanol extracts of the dried bark powder of two medicinally important plants, viz., *Pongamiapinnata* (PP) and *Azadirachtaindica* (AI) and their therapeutic uses. **Method:** UV-visible, FTIR spectral techniques and SEM images were used to characterize the NPs. These bio-NPs were tested for this response against mycobacteria such as Streptomycin and Fluconazole, viruses, bacteria, and fungi. **Results:** Antibacterial activity, antifungal activity and detailed molecular interaction between the therapeutic constituents of PP and AI against Human Mixtard Insulin (HMI) and Histamine were studied by *in silico* docking analysis. The antimicrobial studies of both PP and AI yielded positive results in our attempt to investigate the mycobacterial study against two human pathogenic organisms. **Conclusion:** Extensive *in-silico* docking study showed that the decreasing order of non-covalent interactions of four therapeutic components is Isopongachromene > Karanjin > Quercetin > Azadirachtin against Insulin and Isopongachromene > Azadirachtin > Karanjin > Quercetin against Histamine.

1. Introduction

Several medicinal plants have been employed in the past several years by mankind to mitigate or cure various local diseases throughout the world either by processing naturally the various parts of the plant or by combining their secondary effects into drugs [1]. Various plant parts contain several bioactive compounds.

They belong to alkaloid, steroid, saponin, tannin, glycoside and flavonoid group of organic compounds [2]. The last few centennials have seen a copious upsurge in herbal and medicinal plants. The introduction, development, and advancement of the herbal and medicinal uses of plants in the past decades due to the numerous inventions of basic and

Abbreviations: DPPH, 1,1-diphenyl-2-picrylhydrazyl (DPPH)-2,2-diphenyl-1-picrylhydrazyl; HMI, Human Mixtard Insulin; NPs, Nanoparticles; MHA, Mueller Hinton Agar

*Corresponding author: justin@loyolacollege.edu, justinbaskar@gmail.com

doi:

Received 2 July 2024; Received in revised form 25 May 2025; Accepted 24 June 2025

© 2023. Open access. This article is distributed under the terms of the Creative Commons Attribution-NonCommercial 4.0 International License (<https://creativecommons.org/licenses/by-nc/4.0/>)

sophisticated analytical techniques expanded the medicinal values of the plant extracts [3-5]. It has been recognized by WHO, that nearly 15000 plants of pharmaceutical importance exist in different places throughout the world. Almost 255 drugs were extracted from these plants and several synthetic drugs obtained from the natural resources are considered fundamental and essential drugs by the WHO [6-10]. Due to various adverse effects and the capability of microbes developed by some of the chemically synthesized drugs, humankind became ethno-pharmacognosy [11]. Nearly a few thousand phytochemical components present in the plants were found to be a substitute and considered safe with fewer adverse effects. Parts of plants possess certain antibacterial, anti-inflammatory, antifungal, antioxidant, antidiabetic, antidiarrheal, antimicrobial, anthelmintic, anti-infective, antiulcerogenic, antarthritic, anti-emetic, anti-spasmodic, cytotoxic, anticancer, anti-fertility and radio-protective biological activities [12-15].

In recent years nanotechnology is developed as an important field of scientific development. The development of noble nano-materials has received greater attention and attraction in multidisciplinary fields. This paved path and opportunity for researchers in the different applications of metal nanoparticles [16-18]. Nanoparticles (NPs) are synthesized different methods and physical methods require robust energy and space for synthesizing NPs, and it is quite expensive. Chemically synthesized NPs are not suitable in the field of medicine due to their hazardous binding on the surface [19-21]. Researchers synthesized probe antimicrobial activities. Biosynthesis of NPs is cost-efficient, time-saving, and eco-friendly. Biomolecules in plants like proteins, flavonoids, alkaloids, etc., embedded in synthesized NPs can reduce

various metal ions [22]. The foremost steps to examine the bioactivity of the plant-based components are extraction, pharmacological and phytochemical tests. Besides, instrumental methods like UV-visible, FTIR, and SEM analysis are employed to characterize the organic compounds. Extraction is one of the essential steps in the analysis of medicinal plants as it is useful for reviewing and also to characterize bioactive components [23-26]. In the present work, *PP* and *AI* dried bark powders were extracted using aqueous methanol with a Soxhlet extractor. It is because researchers have reported that leaf extracts obtained by conventional method of heating have limited applications. Hence, we aimed to prepare the AgNPs by a greener method using a sonicator. Subsequently, the aqueous methanolic extract was taken for evaluation and testing antibacterial, antifungal, antioxidant activities and for UV-visible, FTIR, SEM, and *In-Silico* docking studies.

2. Material and Methods

2.1. Plant materials

Barks of *PP* and *AI* used in the present work were from the Southeast region of Tamil Nadu, India. We thank Dr.R.Ravindran, Associate Professor, Department of Plant Biology and Biotechnology, Loyola College (Autonomous), Chennai 600034, India for extensive identification of the two plants. Herbarium number of *AI* is BSI/Bot/1982/11023 Southern Circle Herbarium, Coimbatore, India that of *PP* is BSI/Bot/M/2013/37477 (Fig. 1). AnalR samples were used and the solutions were prepared in conductivity water. They were stored in the dark to keep away from any possible photochemical reactions.

2.2. Preparation of methanolic extract

Collected *PP* and *AI* barks (Fig.1 & 2) were leached with water so that dust and other foreign surface materials and pollutants are removed and dried in a shaded air for nearly 10-15 days to ensure complete removal of the moisture. The bark was cut into pieces, powdered in a mixer and kept in an airtight dark bottle [27]. 10 g of powdered bark was extracted with 70:30 methanol/water using a Soxhlet extractor with a sonicator and dried through a

rotary evaporator. The extract was prepared with minimum volume of methanol and the apparatus called Soxhlet extractor which prevent the direct exposure to either environment or humans. Also, the conventional method of heating was not applied to avoid possible chemical change in the constituents of medicinal importance. Instead, we used sonicator as an effective homogeniser; hence it is a green synthesis.



(a)



(b)

Fig. 1. (a) *Azadirachta indica* (AI) and (b) *Pungamia pinnate* (PP)



(a)



(b)

Fig. 2. (a) *Azadirachta indica* (AI) extract and (b) *Pungamia pinnate* (PP) extract

2.3. Storage of the prepared extracts

Prepared extracts were distinctively labeled and stored in an airtight glass bottle in a dark and cool place at 4°C for further use.

2.4. Percentage of extraction content

Petri dishes were used for evaporating the obtained extracts. The weight of the empty petri dish (W_1) and the weight of the petri dish with

evaporated extracts (W_2) were noted [27]. Using the weights, the percentage of the contents was calculated using the formula:

(1)

$$\% \text{ extract content} = \frac{W_2 - W_1}{\text{Total weight of the bark used}} * 100$$

2.5. Phytochemical Screening using methanolic extracts

The residue of the extracts obtained from each bark was tested for the presence of various phytochemical compounds using standard procedures [28].

2.6. Synthesis of Silver nanoparticles of PP and AI bark extracts

Silver nitrate (Molar mass 170g/mol) solution of concentration 1milli mole per liter and stored in dark used. The extracts of *PP* and *AI* were mixed with 1mM silver nitrate separately in 1:9 ratio and kept aside for 30 min. to get AgNPs. It was centrifuged at 10,000 rpm for 20 min and AgNPs were precipitated. It was then washed with 10 mL conductivity water, centrifuged to remove the surfeit biomass and made into pellets. The pellet of AgNPs was dried in a desiccator for about 12 hours before use.

2.7. Antibacterial activity

Agar well diffusion method in Mueller Hinton Agar (MHA) plates was employed in the antibacterial assay. The test organisms were inoculated in nutrient broth and incubated overnight at 37°C to adjust the turbidity to 0.5 McFarland standards giving a final inoculum of 1.5×10^8 CFU/ml. Cultured MHA plates were standardized using microbial culture broth. The individual well was filled with 50µg/ml, 75µg/ml and 100 µg/ml of the samples with streptomycin as positive control (25 mcg) and DMSO as negative solvent control. The plates were allowed to diffuse for 30 minutes at room

temperature and incubated for 18-24 hours at 37°C. Plates were noted for the formation of a clear zone around the well after incubation. This correlates with the antibacterial activity of the test samples. The zone of inhibition (ZOI) was noticed and studied in mm.

2.8. Antifungal activity

Antifungal assay of various samples was studied by a similar method. The test organisms have been inoculated in nutrient broth at 37°C and incubated overnight to adjust the turbidity to 0.5 McFarland standards which gives inoculum of 1.5×10^8 CFU/ml. MHA plates have been cultured with standardized microbial broth. The well was filled with 50µg/ml, 75µg/ml and 100 µg/ml of the samples, fluconazole as positive control (25 mcg) and DMSO solvent as negative control. The plates were allowed to diffuse at room temperature as in the antibacterial activity study and zone of inhibition measured.

2.9. Antioxidant activity using DPPH Radical

The hydrogen atom or electron donation ability of the components in the extracts was measured using methanol solution diphenyl picryl hydroxyl (DPPH). The spectrophotometric assay utilizes the stable DPPH radical as a reagent [29]. Similar concentrations used in the above two activity assay were added to 5 mL of a 0.004% methanol solution of DPPH and incubated for 30 minutes at room temperature. The absorbance was noted at 517 nm against the blank and IC50 values were calculated for *PP* and *AI* extracts using eqn. (2).

Inhibition % for free radical DPPH calculated using

$$\% A = \frac{(\text{Blank A} - \text{sample A})}{\text{Blank A}} * 1000 \quad (2)$$

In the above equation, blank A is the absorbance of the control reaction and sample A is the absorbance of the test compound.

2.10. UV-visible and FTIR Spectral analyses

The biosynthesis of AgNPs was established by spectral study on the reaction mixture after 24 h of reaction. The formation of NPs was preliminarily validated visually by the color change from yellow to brown. The reduction of silver ions in the solution mixture was confirmed by UV-visible spectroscopy by recording the spectra of synthesized AgNPs in the wavelength of 200 to 600 nm (resolution 2 nm) in a Shimadzu UV-1650 model spectrophotometer. The bioactive components responsible for silver reduction, formation and capping were identified using Fourier Transform Infra-Red (FTIR) spectroscopy (Nicolet is 5, Thermo Scientific) FTIR spectral reading was carried out in the range from 500 to 4000 cm^{-1} at a resolution of 4 cm^{-1} .

2.11. SEM analysis

Morphology, shape, size, and distribution of the AgNPs were analysed by Scanning Electron Microscopy.

2.12. Molecular docking software

Molecular docking is an useful tool in the anti-viral study of bioactive compounds. Though there are several software for docking analysis Autodock4.2 molecular docking software developed by the Scripps Research Institute was used in the present study.

3. Results

3.1. Percentage yield of bark extracts

The barks of PP and AI were extracted using methanol and the yield of the methanolic extracts was found to be 7.1g/100g for PP and 8.96g/100g for AI. These values arrived using the equation (1).

3.2. Phytochemical screening of PP and AI

The presence of various metabolites in the methanolic bark extracts of PP and AI was performed using freshly prepared reagents [30]. The presence of phytochemicals was evidenced from preliminary screening shown in Table 1.

Table 1. Phytochemical screening of various components of methanol extracts

No.	Phytochemical components	Methanolic extract of <i>Pongamia pinnate</i> (PP)	Methanolic extract of <i>Azadirachta indica</i> (AI)
1	Carbohydrates	Molisch test	+
		Fehling's test	+
2	Glycosides	Keller-Kiliani Test	+
		Concentrate H_2SO_4 Test	-
		Bromine water test	-
3	Flavonoids	Ferric chloride test	+
		NaOH test	-
		Ellagic acid test	+
		Dragedroff's test	+
4	Alkaloids	Mayer's reagent	-
		Wagner's reagent	-
		Ferric chloride test	+
5	Tannins	Lead acetate test	+
		Froth	-
6	Saponins		
7	Sterols	Liebermann Bur chard test	+
		Salkowski test	+

+ sign indicates positive response and - sign indicates negative result

3.3. Antibacterial activity

The antibacterial activity of the nanoparticles was determined by measuring the inhibitory concentration values of AgNPs against the bacteria *E. coli* and *S. aureus*. The results are presented in Figs 3 & 4. The concentration of AgNPs which can cause the inhibition of visible growth subjected to three different concentrations of AgNPs such as 50 μ l, 75 μ L and 100 μ L for *PP* and *AI* showed positive antibacterial activity against human pathogenic organisms such as *E. coli* (gram-negative bacteria) and *S. Aureus* (gram-positive bacteria) compared with standard antibiotic streptomycin as in Tables 2 & 3.

3.4. Antifungal activity

It may be pointed out that AgNPs obtained from the extracts of *PP* and *AI* showed positive antifungal activity against the pathogenic organism *C. albicans* and it was compared with standard antibiotic Fluconazole (Figs. 3 & 4). The results are presented in Table 3 for the nanoparticles of *PP*. It is observed that the maximum zone of inhibition observed against the pathogens at concentration 75 μ l is 4 mm in *E. coli*, 5 mm in *S. aureus* and the minimum zone of inhibition is 3 mm for *C. albicans*. For *AI*, the maximum zone of inhibition was observed against the pathogens at 75 μ l concentration as 6mm, and the minimum zone of inhibition at 100 μ l concentration was 2 mm in *C. albicans*.

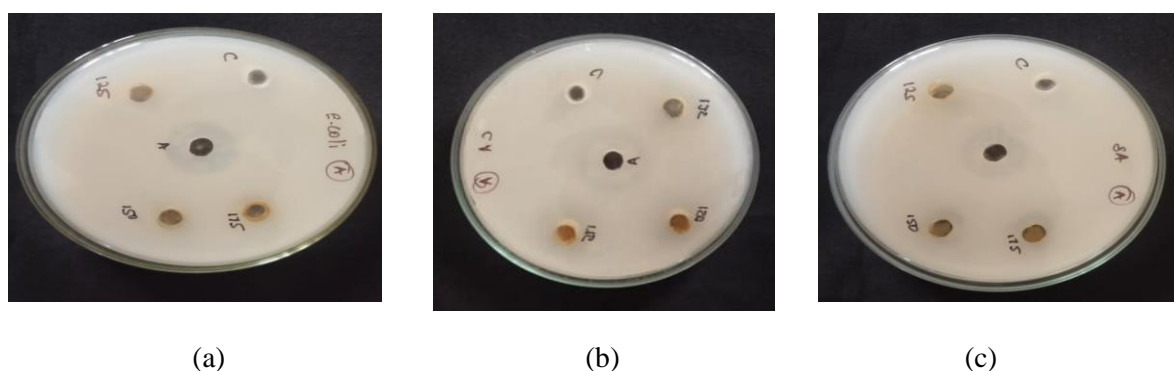


Fig. 3. (a) *E. coli*, (b) *S. aureus* and (c) *C. albicans* bacterial activity for *Pungamiapinnate*

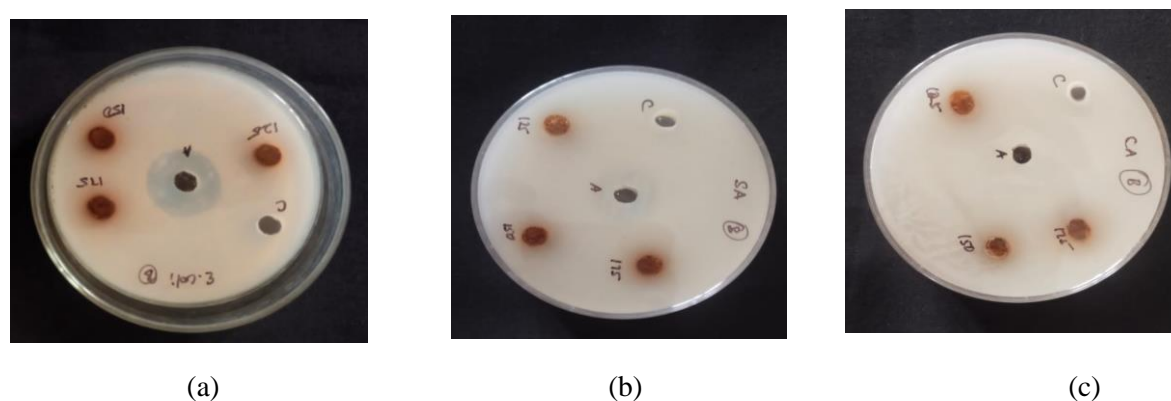


Fig. 4. (a) *E. coli*, (b) *S. aureus* and (c) *C. albicans* bacterial activity for *Azadirachta indica*

Table 2. Antibiotics used for antibacterial and antifungal activities

Control	Antibiotics for bacterial organism	Antibiotics for fungal organism
Sterilized water	Streptomycin	Fluconazole

Table 3. Zone of inhibition of different concentrations of *PongamiaPinnata*.

Organism	<i>Pongamia pinnate (PP)</i>				<i>Azadirachta indica (AI)</i>			
	Zone of inhibition (mm)			Antibiotics	Zone of inhibition (mm)			Antibiotics
	50	75	100		50	75	100	
<i>E. coli</i>	2	4	-	7	5	6	3	7
<i>S. aureus</i>	3	5	-	7	4	6	3	7
<i>C. albicans</i>	2	3	-	6	4	6	2	6

3.4. Antifungal activity

Synthesized AgNPs of *PP* and *AI* showed positive antifungal activity against the pathogenic organism *C. albicans* at three different concentrations 50 µl, 75 µl, and 100 µl by agar well diffusion method with standard antibiotic Fluconazole depicted in Fig. 3 & 4. The results are shown in Tables 2 & 3 for the nanoparticles of *PP*, the zone of inhibition against all the organisms at all the three concentrations 50 µl, 75 µl, and 100 µl respectively. The maximum zone of inhibition observed in diameter(mm) against the pathogens at concentration 75 µl is 4 mm in *E. coli*, 5 mm in *S. aureus* and the minimum zone of inhibition is 3 mm for *C. albicans*. For *AI*, the maximum zone of inhibition was observed against the pathogens at 75 µl concentration as 6mm, and the minimum zone of inhibition at 100 µl concentration was 2mm in *C. albicans*.

3.5. Antioxidant activity

The antioxidant activity is evaluated for different concentrations of biosynthesized AgNPs of *PP* and *AI* (20 µg/mL - 100 µg/mL).

It is observed that the percentage of inhibition increases with an increase in the concentration of the AgNPs extracts as shown in Tables 4 & 5. The efficacy of AgNPs as an oxidant activity increases with an increase in concentration for *PP* and *AI* shown in Fig. 5. Antioxidant activity can be expressed by the IC₅₀ value which is the effective concentration of the extract required to reduce 50% of the totally free radicals. The lower the IC₅₀ value, the more potent the substance is at scavenging DPPH and this implies higher antioxidant activity. The results show that the AgNPs obtained from *PP* extract have higher antioxidant property than those synthesized from the extract of *AI*.

3.6. UV spectral analysis

UV spectral analysis confirmed the formation of AgNPs. It was evident from the results obtained that the extract of *PP* (Fig. 6) and *AI* (Fig. 6) yielded the formation of reduced AgNPs. The peaks between 234-239nm with Gaussian shape in the UV-visible spectra (Fig.6) showed the formation of stable AgNPs.

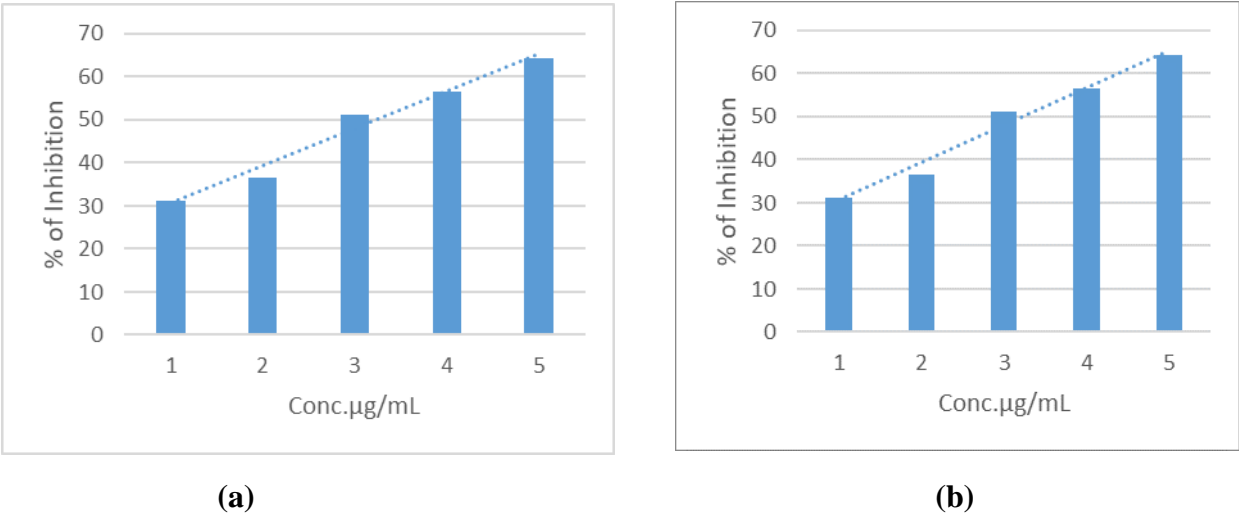


Fig. 5. Bar diagram of antioxidant efficacy of AgNPs using DPPH method for *Pongamia pinnata* (a) and *Azadirachta indica* (b)

Table 4. Antioxidant assay of % inhibition for *Pongamia pinnata* (PP)

Conc. µg/mL	I	II	III	Avg.	% of Inhibition
20	0.060	0.062	0.065	0.062	31.11
40	0.056	0.058	0.057	0.057	36.67
60	0.045	0.046	0.043	0.044	51.11
80	0.040	0.039	0.038	0.039	56.67
100	0.030	0.031	0.034	0.032	64.44
IC ₅₀					58.5

Table 5. Antioxidant assay of % inhibition for *Azadirachta indica* (AI)

Conc. µg/mL	I	II	III	Avg.	% of Inhibition
20	0.058	0.060	0.061	0.060	33.33
40	0.050	0.055	0.057	0.054	40.00
60	0.042	0.041	0.046	0.042	53.33
80	0.039	0.035	0.035	0.036	60.00
100	0.030	0.029	0.032	0.030	66.66
IC ₅₀					63.55

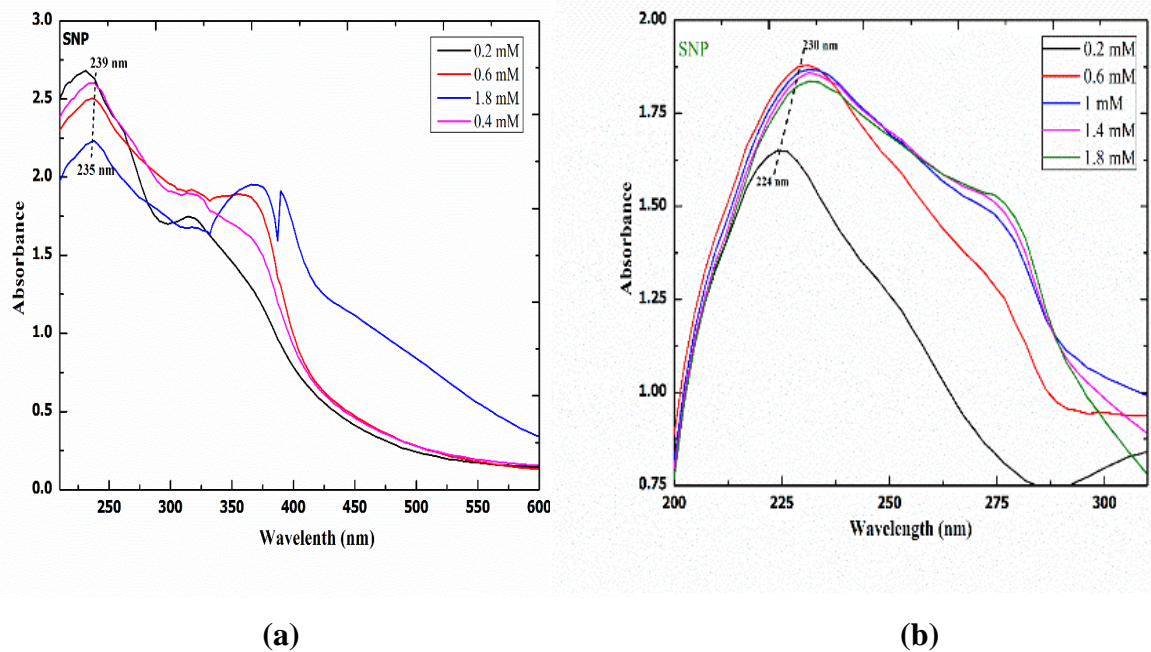


Fig. 6. UV–vis spectra of different solutions involved in the biosynthesis of the AI (a) and (b) PP-AgNPs colloid. Increasing the peak intensity with time, along with a clear red shift indicates the synthesis of stable silver nanoparticles during the processing time.

3.7. FT-IR analysis

AgNPs obtained from bark extracts of PP (A) and AI (B) were characterized by FT-IR spectra. The prominent bands observed around 457.56 cm^{-1} to 1292.5 cm^{-1} are shown in Table 6. The observed peaks show the presence of alkyl halides, amines, C-O in hydroxyl groups, alkyl ketone, carboxylic acid group, phenols, (O-H stretching vibrations bands), secondary O-H groups show the presence of compounds like flavonoids, terpenoids, glycosides, alkaloids. These compounds are responsible for efficient capping and stabilization of AgNPs. FT-IR spectra are depicted in Figs. 7 & 8.

Table 6. Frequencies of vibration modes of certain groups observed in FTIR spectra of methanol extracts

S.No	Vibrational mode	$\nu\text{ cm}^{-1}$
1	C-X (Halogen)	457.56
2	C-X (Halogen)	492.11
3	C-X (Halogen)	528.83
4	= C-H	611.62
5	C-O str	1108
6	C-C str (ketone)	1292.5
7	N=C=S	2026
8	-C≡N(Nitriles)	2344
9	O-H str	3204
10	O-H str	3534.7
11	O-H str	3856.7

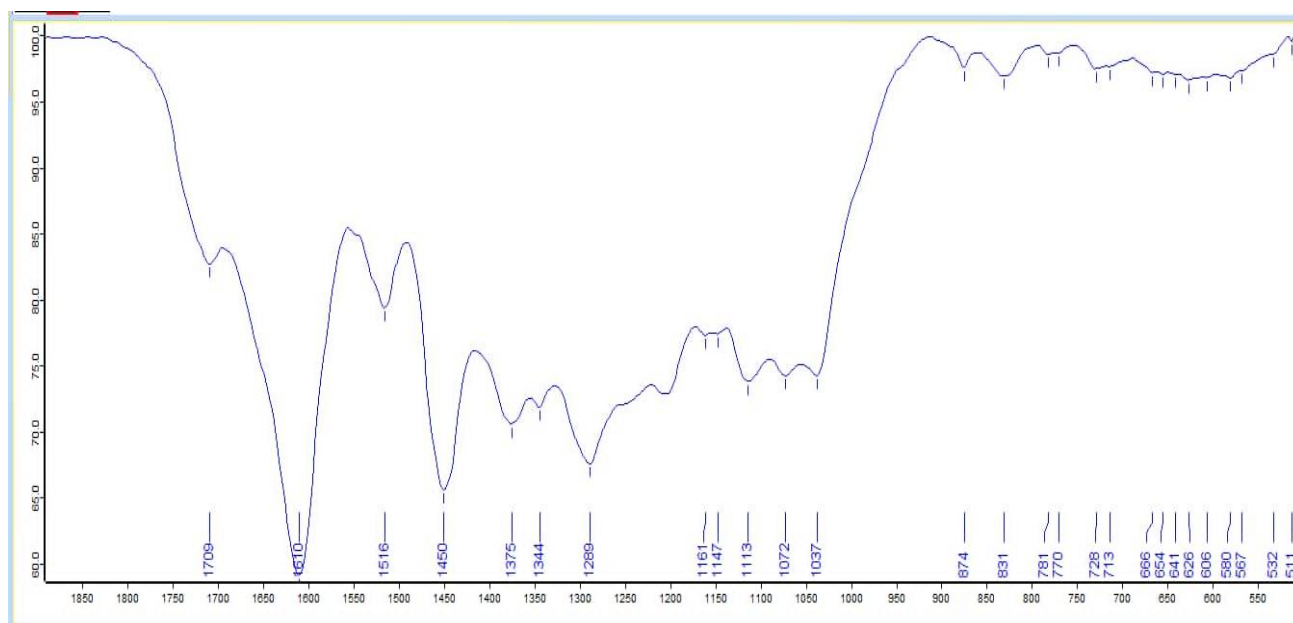


Fig. 7. FT- IR Spectrum of methanolic extract of *Azadirachta indica*

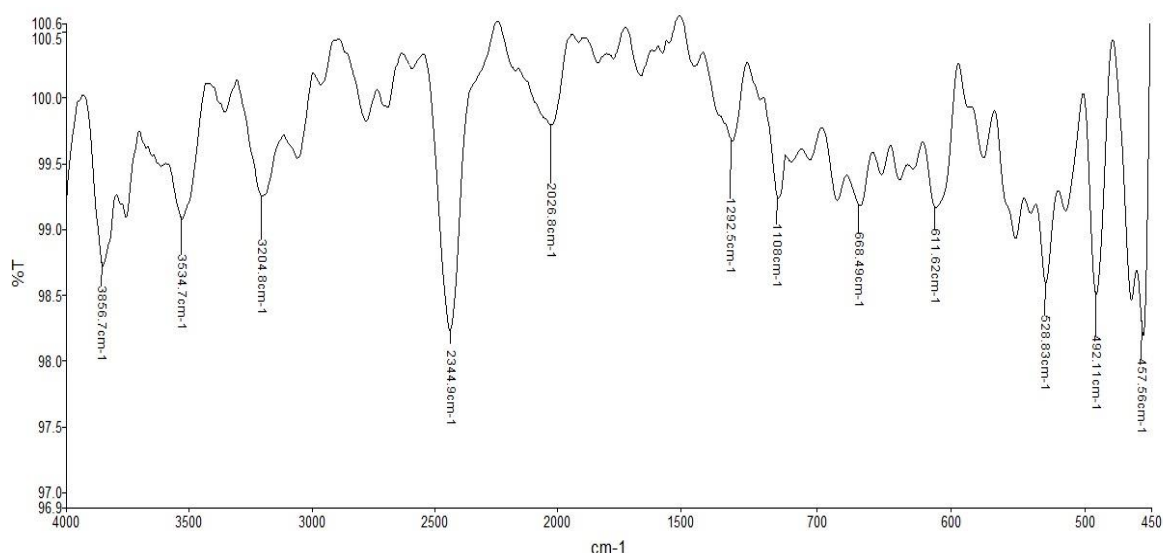


Fig. 8. FT- IR Spectrum of methanolic extract of *Pungamia pinnate*

3.8. SEM analysis

SEM photographs of AgNPs synthesized from the extracts of PP and AI show the morphology of AgNPs at a magnification 500x, reduced voltage acceleration at of 30kv for AI and magnification at 1000x, voltage acceleration of 30kv for PP are shown in Fig. 9(a) and 9(b)

respectively. These images show that the morphology of the AgNPs has a non-uniform and irregular particle size [31]. The random shape and size may be due to the agglomeration of the formed nanoparticles of the bark silver extract (Fig. 9).

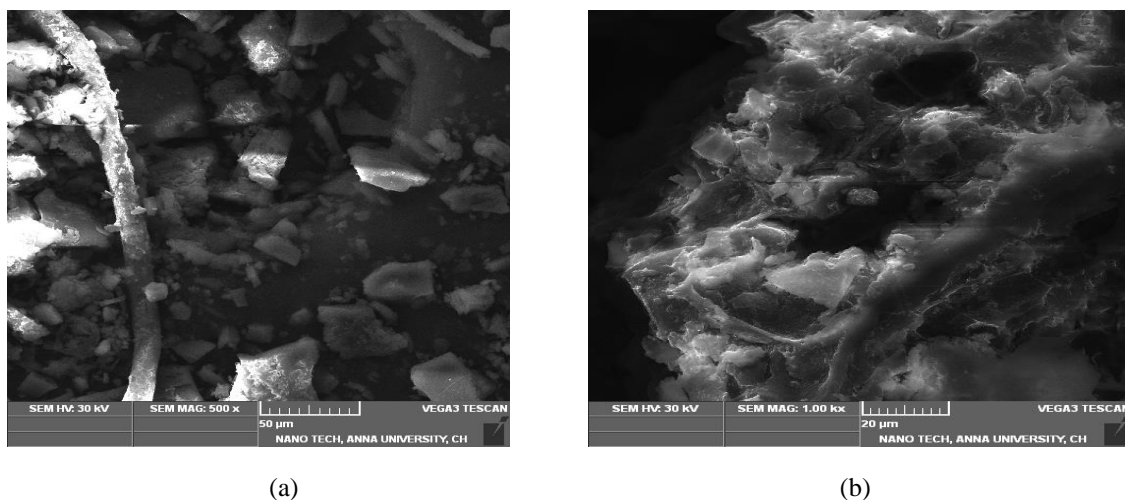


Fig. 9. SEM image of (a) *Azadirachta indica* and (b) *Pongamia pinnate*

3.9. In-Silico molecular docking analysis

The molecular interaction between the chief therapeutic component of *PP* and *AI* (Fig. 10) against Human Mixtard Insulin (HMI) and Histamine is investigated by in-silico docking studies. This kind of analysis could help us to understand how far the phytochemicals will affect the metabolic function of human mixture insulin (HMI) [32]. Since ancient times, *AI* has been used as a natural medicine for many diseases like antiallergic, antitoxic antidiabetic, antibacterial, and antifungal activity etc. Antidiabetic activity may be due to the interaction of therapeutic active components of *AI* like Azadirachtin and Quercetin against Insulin and its antiallergic activity may be due

to its bioactive components of *PP* like Isopongachromene and Karanjin against histamine of the body's cells which causes many of the symptoms of allergies. Therefore, the understanding of the strength of molecular interaction between the chief therapeutic components of *PP* and *AI* may bring the attention of the clinicians of Ayurvedic medicines. Therefore, an attempt was made to assess the strength of molecular interactions between the therapeutic components of *AI* and *PP* with Insulin and Histamine by In-Silico docking analysis. In this regard, we have performed the molecular docking analysis using *Autodock 4.2*, and the results obtained are presented in Tables 7 & 8.

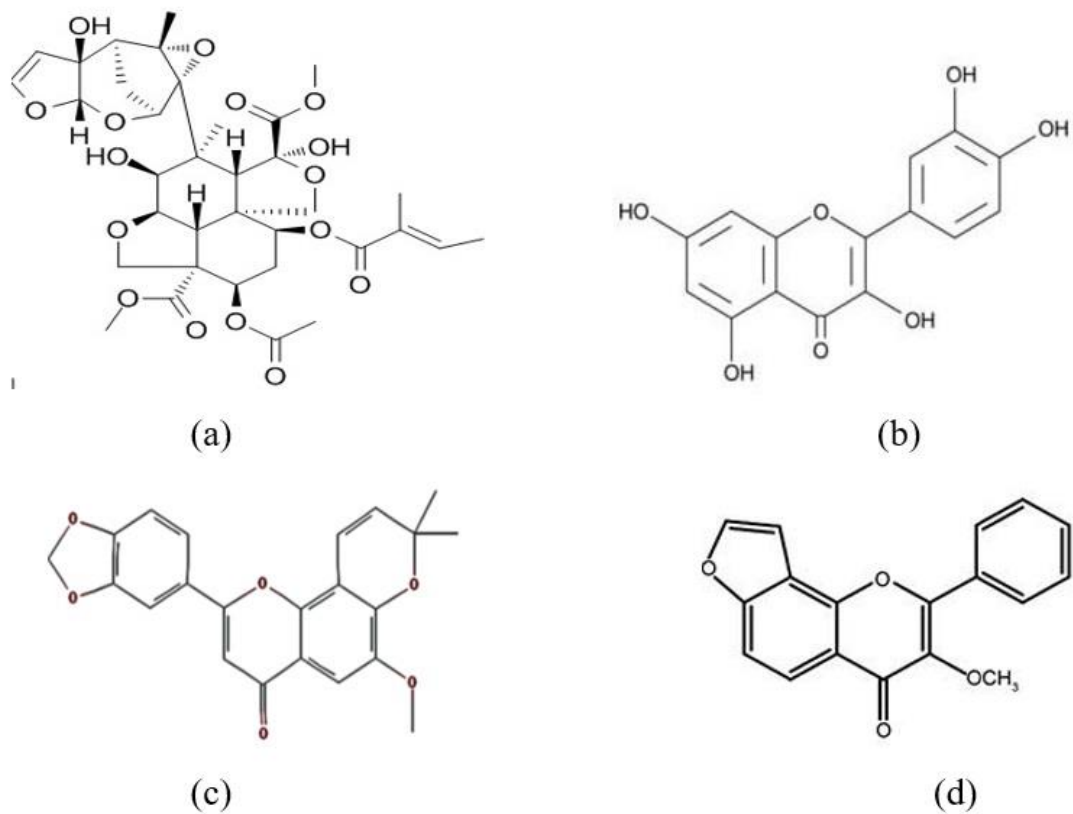


Fig. 10. Structures of chief phytoconstituents of *Azadirachta indica* such as (a) Azadirachtin, (b) Quercetin and *Pongamia pinnate* such as (c) Isopongachromene (d) Karanjin bark extracts.

Table 7. Molecular docking results of human mixtard insulin (HMI) with therapeutic constituents of *Azadirachta indica* (AI) and *Pongamia pinnata* (PP) bark extracts.

Plant name	Chief phytoconstituents	Molecular mass In Dalton	Binding energy (k cal/mol)	Inhibition constant (Ki)/uM	vdW+Hbond+ Desolv energy (k cal/mol)	Final intermolecular energy (k cal/mol)	Final total internal energy (k cal/mol)	Torsional free energy (k cal/mol)
<i>Azadirachta indica</i>	Azadirachtin	720.7	-6.04	37.50	-9.92	-9.92	+0.00	+3.88
	Quercetin	302.2	-6.65	13.36	-8.44	-8.44	+0.00	+1.79
<i>Pongamia pinnata</i>	Karanjin	292.3	-6.62	14.09	-7.21	-7.21	+0.00	+0.60
	Isopongachromene	378.4	-7.52	3.08	-8.12	-8.12	+0.00	+0.60
	HMI	5700	-	-	-	-	-	-

Table 8. Molecular docking results of aqueous histamine H1 receptor with therapeutic constituents of *Azadirachta indica* and *Pongamia pinnata* bark extracts.

Plant name	Chief phytoconstituents	Molecular mass In Dalton	Binding energy (k cal/mol)	Inhibition constant (Ki)/uM	vdW+Hbond+ Desolv energy (k cal/mol)	Final intermolecular energy (k cal/mol)	Final total internal energy (k cal/mol)	Torsional free energy (k cal/mol)
<i>Azadirachta indica</i>	Azadirachtin	720.7	-7.74	2.12	-13.11	-13.11	+0.00	+5.3
	Quercetin	302.2	-6.26	25.66	-8.05	-8.05	+0.00	+1.79
<i>Pongamia pinnata</i>	Karanjin	292.3	-6.50	17.33	-7.09	-7.09	-0.81	+0.6
	Isopongachromene	378.4	-7.83	1.82	-8.43	-8.43	+0.00	+0.6
Histamine H1			-	-	-	-	-	-

It is observed from the docking analysis that the binding energy of the chief therapeutic components of *AI* such as Azadirachtin and Quercetin have $-7.74\text{kcal mol}^{-1}$ and $-6.26\text{kcal mol}^{-1}$ respectively against Histamine and $-6.04\text{kcal mol}^{-1}$ and $-6.65\text{kcal mol}^{-1}$ respectively against Insulin. The chief therapeutic components of *PP* such as Isopongachromene and Karanjin have $-7.83\text{kcal mol}^{-1}$ and $-6.50\text{kcal mol}^{-1}$ respectively

against Histamine and $-7.52\text{kcal mol}^{-1}$ and $-6.62\text{kcal mol}^{-1}$ respectively against Insulin. The high binding energy is largely attributed to the existence of various types of non-covalent interactions such as van der Waals and hydrogen bonded interactions. The two-dimensional structure depicting molecular interactions between Azadirachtin and insulin, Azadirachtin, and histamine are given in Fig. 11 & Fig. 15.

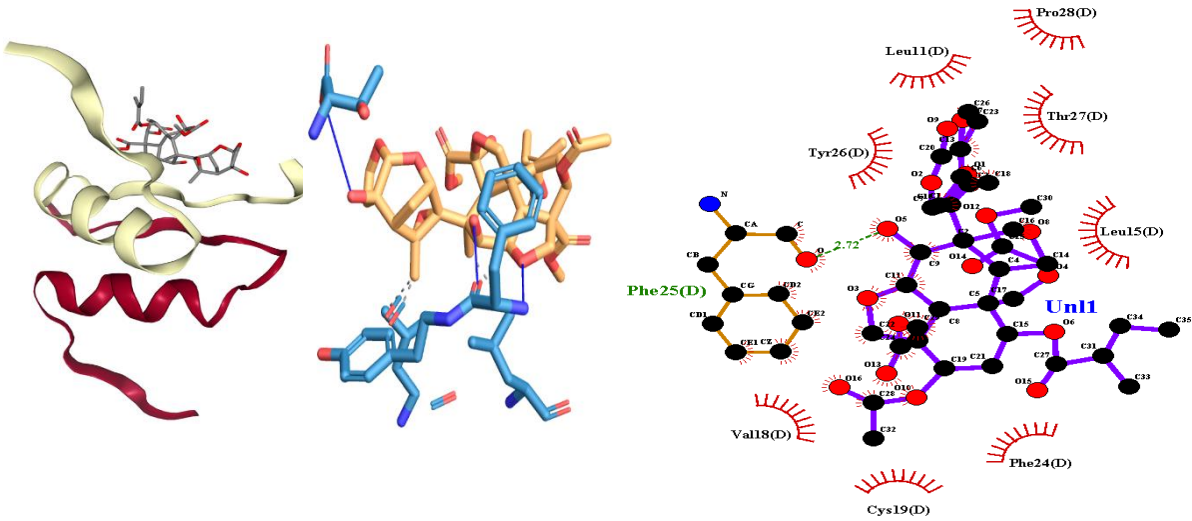


Fig. 11. The interaction between human mixtard insulin (HMI) and Azadirachtin

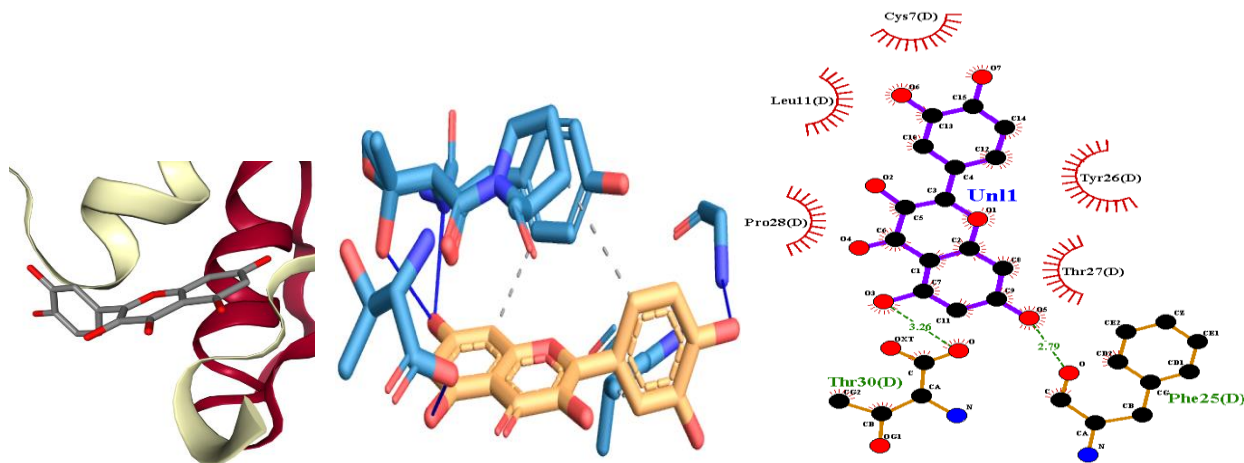


Fig. 12. The interaction between human mixtard insulin (HMI) and Quercetin

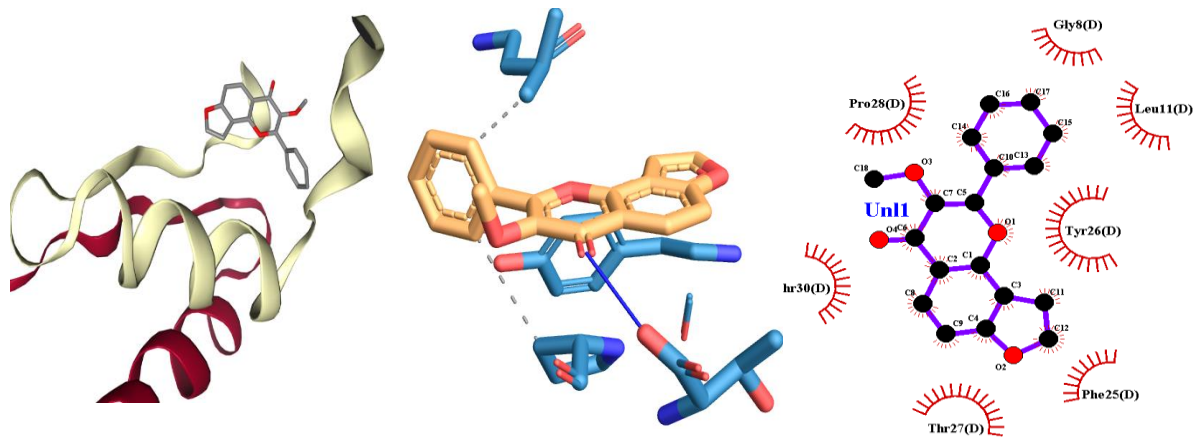


Fig. 13. The interaction between human mixtard insulin (HMI) and Karanjin

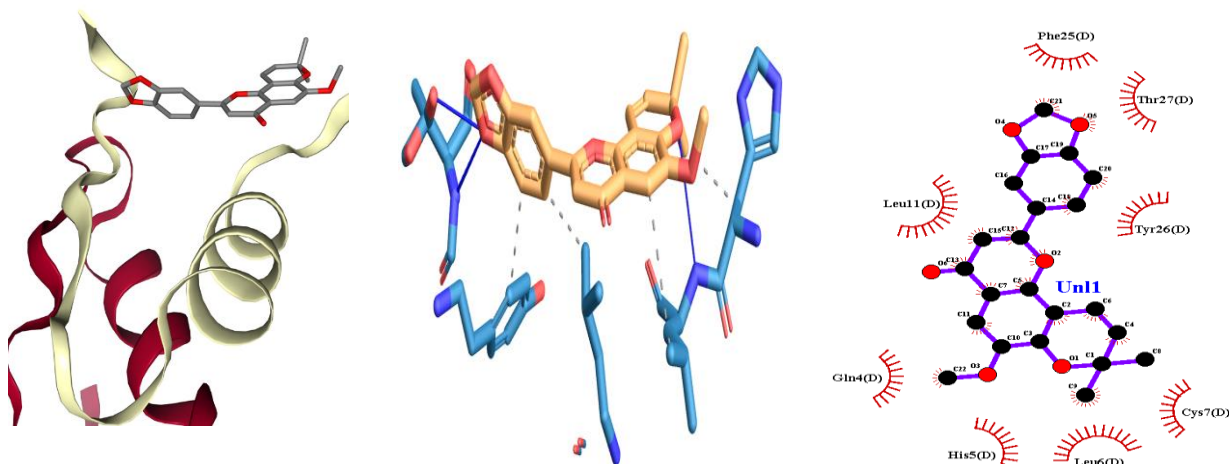


Fig. 14. The interaction between human mixtard insulin (HMI) and Isopongachromene

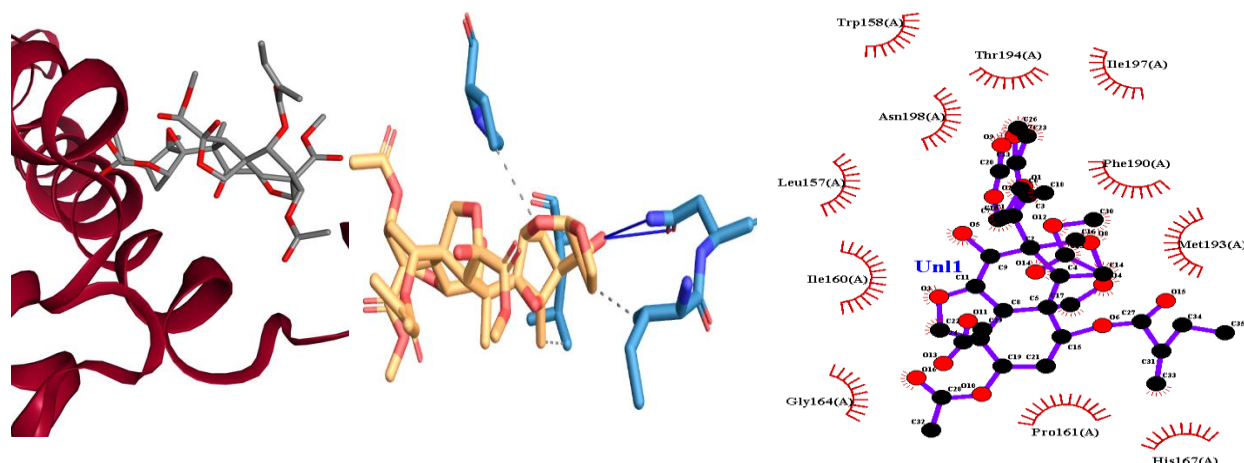


Fig. 15. The interaction between histamine and Azadirachtin

4. Discussion

Based on our preliminary results, it is found that the highest binding energy compound namely Azadirachtin with Histamine has eleven hydrophobic (Trp158(A), Thr194(A), Ile197(A), Ile160(A), Asn198(A), Phe190(A), Met193(A), His167(A), Pro161(A), Gly164(A), and Leu157(A)) and no hydrogen bond interactions whereas Azadirachtin with Insulin has eight hydrophobic (Pro28(D), Leu11(D), Thr27(D), Tyr26(D), Leu15 (D), Phe24(D), Cys19(D) and Val18(D)) and one hydrogen bond (Phe25(D)) interactions. Similarly, the other therapeutic component of AI such as Quercetin with Histamine has five hydrophobic (Gly1107(A), Gli1108(A), Val1103(A), Glu1011(A), Leu1032(A), His1031(A), Asp1070(A), Ala1074(A) and Phe1104(A)) and five hydrogen bond (Glu1108(A), Val1103(A), Glu1011(A), Gly1030(A) and Asp1070(A)) interactions whereas Quercetin with Insulin has five hydrophobic (Cys7(D), Tyr26(D), Thr27(D), Phe25(D), Thr30(D), Pro28(D) and Leu11(D) and two hydrogen bond (Phe25(D) and Thr30(D)) interactions.

The therapeutic components of PP such as isopongachromene against histamine has nine

hydrophobic (Thr147(A), Ala146(A), Gly150(A), Leu154(A), Leu201(A), Phe119(A), Phe116(A), Pro202(A) and Ile120(A)) and no hydrogen bond interactions whereas Isopongachromene against Insulin has eight hydrophobic (Phe25(D), Thr27(D), Tyr26(D), Cys7(D), Leu6(D), Leu11(D), His5(D) and Gln4(D)) and no hydrogen bond. Similarly, the other constituent of PP, Karanjina against Histamine has seven hydrophobic (Phe156(A), Trp152(A), Leu149(A), Ile148(A), Ser68(A) and Val67(A) and no hydrogen bond interactions whereas Karanjina with Insulin also has seven hydrophobic (Gly8(D), Leu11(D), Ty26(D), Phe25(D), Thr27(D), Thr30(D) and Pro28(D)) and has no hydrogen bond interactions. The four chief constituents of both AI and PP have hydrophobic and hydrogen-bonding interactions. The high binding activity in Azadirachtin is due to large number of hydrophobic interactions. The results obtained in docking studies reveal that all four therapeutic components interact significantly with hydrophilic residues of both insulin and histamine. The 2D diagrams of all the complexes with their interacting residues are shown from Figs. 11 - 20. The docking results

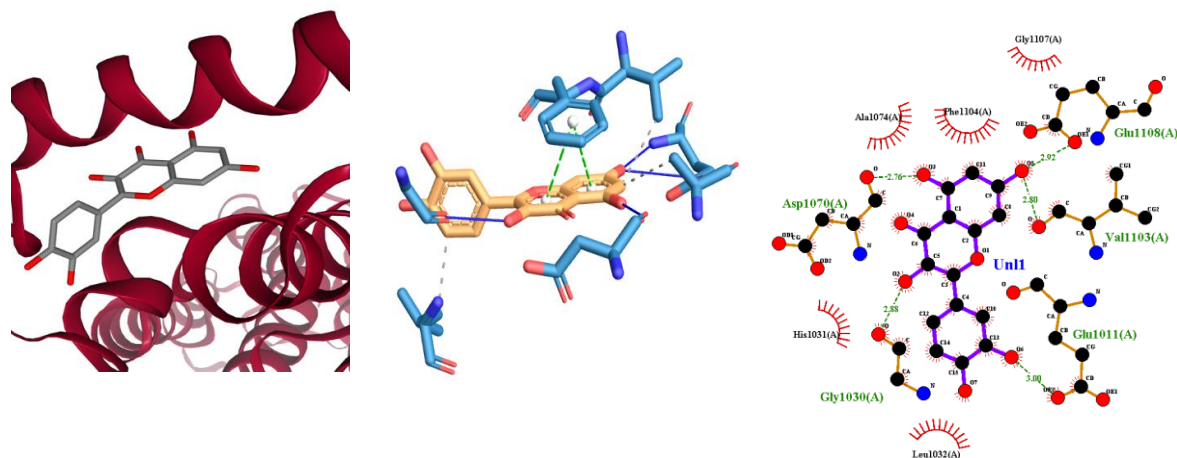
suggest that the binding of therapeutic components with insulin and histamine is not specifically dependent on electrostatic interactions; other bonded and non-bonded interactions are also playing a significant role, which in turn provide high negative binding energy values and lower K_i value for isopongachromene. Thus, docking results show that the order of non-covalent interactions between insulin and four therapeutic components is in the decreasing order:

Isopongachromene > Karanjin > Quercetin > Azadirachtin.

Similarly non-covalent interactions between histamine and four therapeutic constituents is in the decreasing Order:

Isopongachromene > Azadirachtin > Karanjin > Quercetin.

Thus, docking results establish that the therapeutic components of both *PP* and *AI* interact significantly with Insulin against Histamine in the human system.



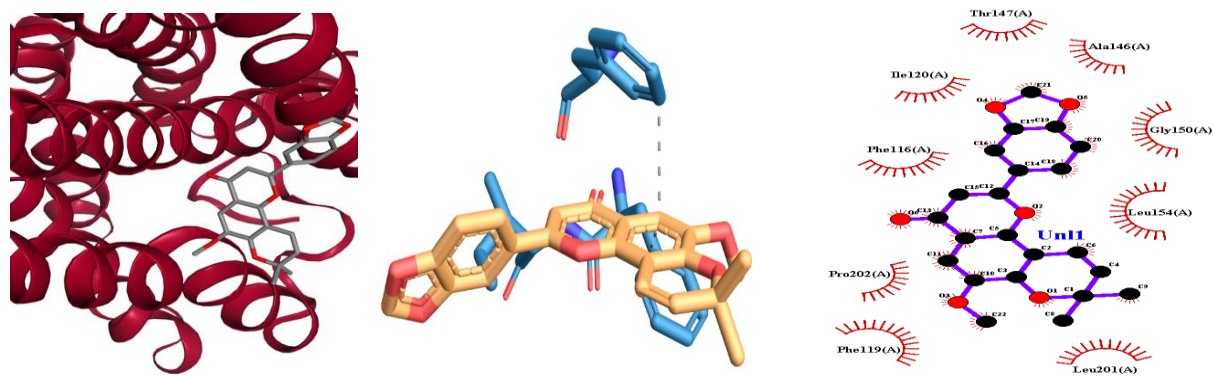


Fig. 18. The interaction between histamine and isopongachromene

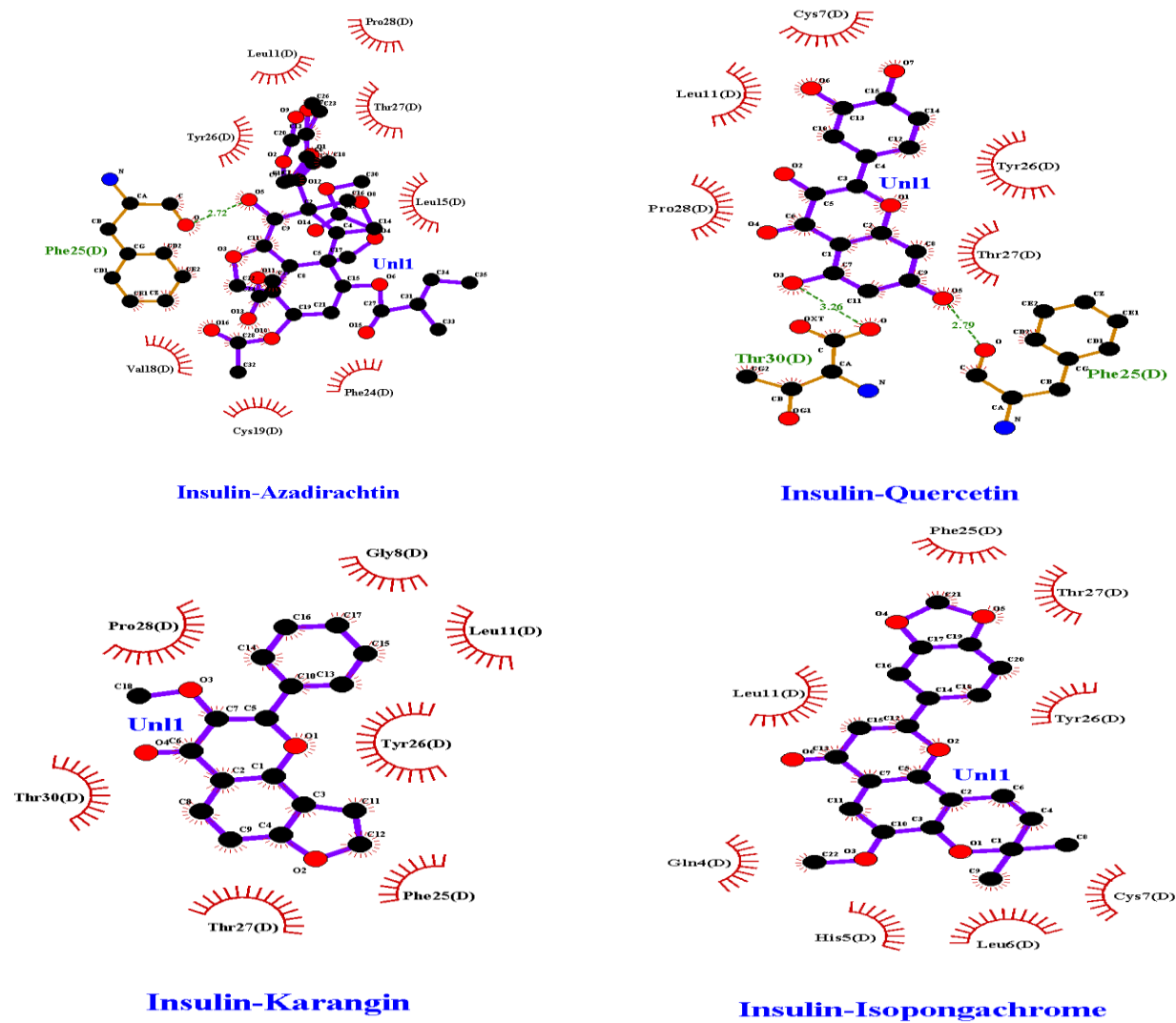
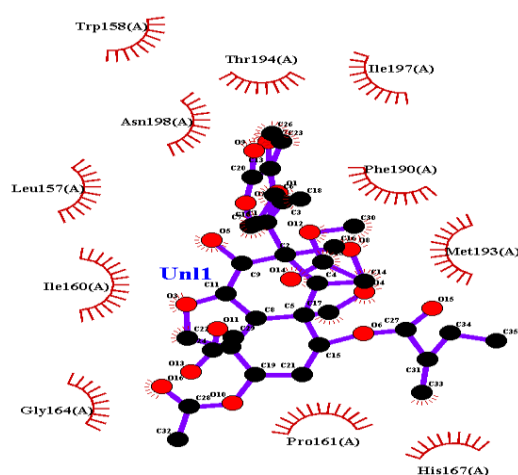
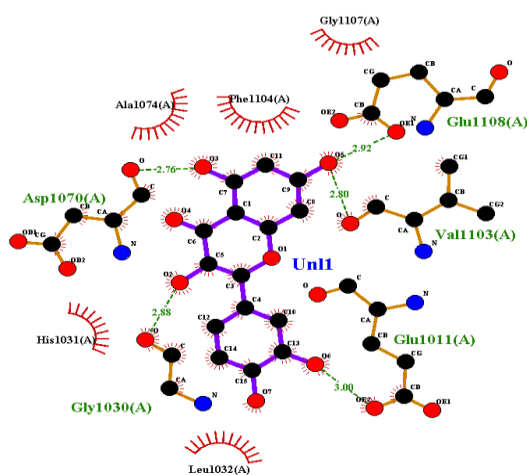


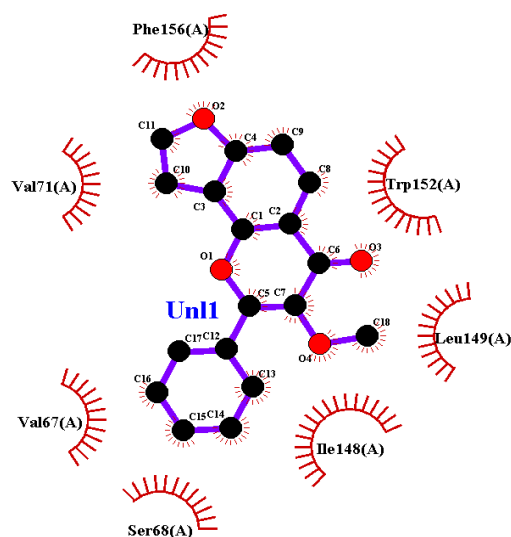
Fig. 19. The interaction between human mixtard insulin (HMI) and the chief phytoconstituents of *Azadirachta indica* and *Pongamia pinnate* bark extracts systems. Hydrogen bond interactions and their distances are highlighted in green colour and hydrophobic interactions and their residues are highlighted in red lines.



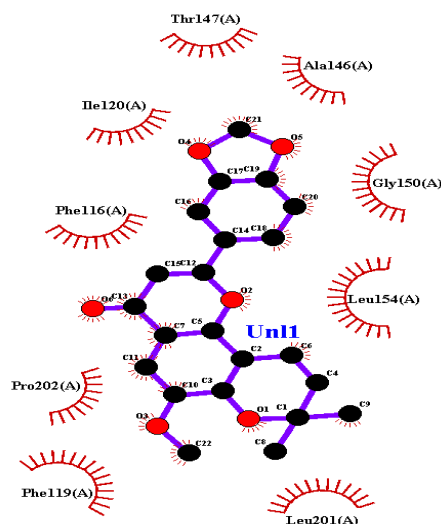
Histamine-Azadirachtine



Histamine-Quercetin



Histamine-Karangin



Histamine-Isopongachromene

Fig. 20. The interaction between histamine H1 receptor and the chief phytoconstituents of *Azadirachta indica* and *Pongamia pinnate* bark extracts systems. Hydrogen bond interactions and their distances are highlighted in green colour and hydrophobic interactions and their residues are highlighted in red lines.

4. Conclusion

The present work reports the preparation of AgNPs in methanol extracts of two medicinal plants, viz., *Pongamia pinnata* (PP) and *Azadirachta indica* (AI) and study of their therapeutic uses. Two synthesized AgNPs were

screened for anti-mycobacterial, antiviral, and antimicrobial activities and characterized by UV-visible spectroscopy, and FTIR analysis to identify the biomolecules responsible for bio-reduction of silver ion. SEM images showed the morphology of the formed silver nanoparticles

size ranges at 20µm and 50µm. Antibacterial activity was done by the Agar well diffusion method, antifungal activity by the disc well method, antioxidant activity by DPPH radical, and the molecular interactions study between the therapeutic components of *PP* and *AI* with Insulin and Histamine by In-Silico docking analysis. The phytochemical analysis was also carried out to understand the presence of various active principles both *PP* and *AI*. The antimicrobial studies of both *PP* and *AI* showed positive antibacterial activity against human pathogenic organisms such as *Escherichia coli* (gram-negative bacteria) and *Staphylococcus aureus* (gram-positive bacteria) compared with standard antibiotic streptomycin. Both *PP* and *AI* AgNPs showed significant antibacterial and antioxidant activity. In-silico docking analysis revealed that the decreasing order of non-covalent interactions of all four therapeutic components is Isopongachromene > Karanjin > Quercetin > Azadirachtin against Insulin and Isopongachromene > Azadirachtin > Karanjin > Quercetin against Histamine.

Acknowledgements

The authors thank the Management Committee of Loyola College, Chennai-600034, and the Management of SDNB Vaishnav College for Women, Chennai-600 044, India for

providing their support and providing necessary facilities to complete the project.

Author contributions

The following is the contribution of the authors: 1. Mulaguri Susairaj Veena Anasthasia- Synthesis of bio-nanomaterials and Phytochemical Screening; 2. Chochalingam Mansiya- Study of antimicrobial activities; 3. Venu Kannappan- Analysis and interpretation of UV-Visible, IR, spectra and SEM; 4. Arulanandu Justin Adaikala Baskar- In-Silico Docking Analysis & Complete manuscript Preparation; We, all the authors, declare that the above-mentioned work is the author's contribution in this research work.

Conflicts of interest

We, all the authors, declare that there is no conflict of interest in our research work.

Funding Declaration

We, the authors, declare that we didn't get any financial assistance from any funding agency. We availed the facilities of two institutions and the management committee of the two colleges are acknowledged in the ' Acknowledgement section of the manuscript.

References

1. Gupta A, Naraniwal M and Kothari V. Modern extraction methods for preparation of bioactive plant extracts. *Inter. J. Appl. Nat. Sci.* 2012; 1(1): 8-26.
2. Sheel R, Nisha K and Kumar J. Preliminary Phytochemical screening of methanolic extract of *Clerodendron fortuneatum*. *J. App. Chem.* 2014; 2278-5736; 7: 10-13. doi: 10.9790/5736-07121013.
3. Fitzgerald M, Heinrich M and Booker A. Medicinal plant analysis: A historical and regional discussion of emergent complex techniques. *Front Pharmacol.* 2020; 10: 1480-1487. doi: 10.3389/fphar.2019.01480.
4. Gupta A, Naraniwal M and Kothari V. Modern extraction methods for preparation of bioactive plant extracts. *Inter. J. Appl. Nat. Sci.* 2012; 1(1): 8-26.

5. Balandrin MF, Klocke JA, Wurtele ES and Bollinger WH. Natural plant chemicals: sources of industrial and medicinal materials. *Science*. 1985; 228(4704): 1154-60. doi: 10.1126/science.3890182.
6. Houghton PJ and Raman A. Laboratory Handbook. Fractionation of Natural Extracts. Chapman and Hall. London, UK, 1998, 39-47.
7. Mutalib LY and Naqishbandi AM. Antibacterial and phytochemical study of Iraqi *Salvia officinalis* leave extracts. *Iraqi J. Pharm. Sci.* 2012; 21(1) 93-97. doi: 10.31351/vol21iss1pp93-97.
8. Khan M, Wassilew S.W, Schmutterer H and Asher K. R. S. Natural Pesticides from the Neem Tree and Other Tropical Plants, GTZ, Eschborn, 1987, 645-650.
9. Sasidharan S, Chen Y, Saravanan D, Sundram MK and Latha L. Extraction, isolation and characterization of bioactive compounds from plants' extracts. *Afr. J. Tradit. Complement. Altern. Med.* 2011; 8(1): 1-10. doi: 10.4314/ajtcam.v8i1.60483.
10. Fabricant D. S and Farnsworth N.R. The value of plants used in traditional medicine for drug discovery. *Environ. Health Perspect.* 2001; 109: 69-75. doi: 10.1289/ehp.01109s169.
11. Duraipandian V, Ayyanar M and Ignacimuthu S. Antimicrobial activity of some ethnomedicinal plants used by Paliyar tribe from Tamil Nadu, India. *BMC Complement. Altern. Med.* 2006; 6: 35-42. doi: 10.1186/1472-6882-6-35.
12. Cos P, Vlietinck AJ, Dirk DV and Maes L. Anti-infective potential of natural products: How to develop a stronger in vitro 'proof-of-concept'. *J. Ethnopharmacol.* 2006; 106(3): 290-302. doi: 10.1016/j.jep.2006.04.003.
13. Dahiru D, Onubiyi J. A and Umaru H. A. Phytochemical screening and antiulcerogenic effect of *Moringa oleifera* aqueous leaf extract. *Afr. J. Trad. Comple. Altern. Med.* 2006; 3(3): 70-75. doi: 10.4314/ajtcam.v3i3.31167.
14. Hazra KM, Roy RN, Sen SK and Laskar S. Isolation of antibacterial pentahydroxy flavones from the seeds of *Mimosa elengi* Linn. *Afr. J. Biotech.* 2007; 6(12): 18: 1446-1449.
15. Parekh J, Karathia N and Chanda S. Evaluation of antibacterial activity and phytochemical analysis of *Bauhinia variegata* L. bark. *Afr. J. Biomed. Res.* 2006; 9(1): 53-56. doi: 10.4314/ajbr.v9i1.48773.
16. Velusamy P, Das J, Pachaiappan R, Vaseeharan B and Pandian K. Greener approach for synthesis of antibacterial silver nanoparticles using aqueous solution of neem gum (*Azadirachta indica* L.). *Indus. Crops and Prod.* 2015; 66: 103-109. doi: 10.1016/j.indcrop.2014.12.042.
17. Narayanan KB and Sakthivel N. Biological synthesis of metal nanoparticles by microbes. *Advances in Colloid and Interface Sci.* 2010; 156: 1-13. doi: 10.1016/j.cis.2010.02.001.
18. Velusamy P, Kumar GV, Jeyanthi V, Das J and Pachaiappan R. Bio-Inspired green nanoparticles: synthesis, mechanism, and antibacterial application. *Toxicol. Res.* 2016; 32(2): 95-102. doi: 10.5487/TR.2016.32.2.095.
19. Bawskar M, Chandrakant S, Gaikwad S, Avinash I, Rathod D, Gade A, Duran N, D. Marcato P and Rai M. A New Report on Mycosynthesis of Silver Nanoparticles by *Fusarium culmorum*. *Current Nanoscience* 2010; 6(4): 376-380. doi: 10.2174/157341310791658919.
20. Ouda SM. Antifungal Activity of Silver and Copper nanoparticles on two plant pathogens. *Res. J. Microbio.* 2014; 9(1): 34-42. doi: 10.3923/jm.2014.34.42.
21. Wei X, Luo M, Li W, Yang L, Liang X, Xu L, Kong P and Liu H. Synthesis of silver nanoparticles by solar irradiation of cell-free

- Bacillus amyloliquefaciens extracts and AgNO₃. *Bioresour. Technol.* 2012; 103(1): 273-281. doi: 0.1016/j.biortech.2011.09.118.
- 22.** Kamiar Zomorodian, Seyedmohammad Pourshahid, Arman Sadatsharifi, Pouyan Mehryar, Keyvan Pakshir, Mohammad Javad Rahimi, Ali Arabi Monfared. Biosynthesis and Characterization of Silver Nanoparticles by Aspergillus Species. *Biomed. Res. Int* 2016; 5435397. doi: 10.1155/2016/5435397.
- 23.** Padalia H, Moteriyia P and Chanda S. Green synthesis of silver nanoparticles from marigold flower and its synergistic antimicrobial potential. *Arab. J. Chem.* 2014; 8(5): 732-741. doi: 10.1016/j.arabjc.2014.11.015.
- 24.** Pandikumar P, Chellappandian M, Mutheeswaran S and Ignacimuthu S. Consensus of local knowledge on medicinal plants among traditional healers in Mayiladumparai block of Theni District, Tamil Nadu, *Ind. J. Ethnopharmacol.* 2011; 134(2): 354-62. doi: 10.1016/j.jep.2010.12.027.
- 25.** Parashar U. K, Saxena P. S, Anchal Srivastava. Bio-inspired synthesis of silver nanoparticles. *Digest J. Nanomat. and Biostructures.* 2009; 4(1): 159-166.
- 26.** Pileni M P. Nanosized particles made in colloidal assemblies. *American Chemical Society*, 1997; *Langmuir*. 13: 3266-3276. doi: 10.1021/la960319q.
- 27.** Bendigeri S, Das G, Shrman K, Kumar S, Khare R. K, Sachan S and Saiyam R. Phytochemical analysis of *Saraca asoca* bark and *Azadirachta indica* seeds. *Inter. J. Chem. Studies.* 2019; 7(4): 126-131.
- 28.** Owoseni, Abimbola A, Ayanbamiji T. A, Ajayi, Yejide O and Ewegbenro Ikeoluwa B. Antimicrobial and phytochemical analysis of leaves and bark extracts from *Bridelia ferruginea*. *African J. Biotechnol.* 2010; 9(7): 1031-1036. doi: 10.5897/AJB09.1072.
- 29.** Küçükgül G, Kocatepe A, De Clercq E, n Şahin F and Güllüce M. Synthesis and biological activity of 4-thiazolidinones, thiosemicarbazides derived from diflunisal hydrazide. *Euro. J. Med. Chem.* 2006; 41(3): 353-359. doi: 10.1016/j.ejmech.2005.11.005.
- 30.** Tiwari P, Kumar B, Kaur M, Kaur G and Kaur H. Phytochemical screening and Extraction: A Review. *International Pharmaceutica Scientia.* 2011; 1(1): 98-108.
- 31.** Taba P, Parmitha N. Kasim S. Sintesis nanopartikel perak menggunakan ekstrak daun salam (*Syzygium polyanthum*) sebagai bioreduktor dan uji aktivitasnya sebagai antioksidan. *Indo. J. Chem. Res.* 2019; 7(1): 51-60. doi: 10.30598/ijcr.2019.7-ptb.
- 32.** Baskar JA, Kulanthaisamy A, Singh DP and Kan-nappan V. Assessing non-covalent interaction between insulin and some antibiotics in aqueous solution through ultrasonic studies and in silico docking analysis. *J. Mol. Liq.* 2016; 224: 1131-1141. doi: 10.1016/j.molliq.2016.10.051.

How to cite this article: Anasthasia MSV, Mansiya C, Kannappan V, AdaikalaBaskar AJ. Synthesis, characterization, anti-microbial activity of silver nanoparticles, and molecular interaction studies of therapeutic agents of *Pongamia pinnata* (PP) and *Azadirachta indica* (AI). *Journal of Medicinal Plants* 2025; 24(94): 81-101.
doi: